# Part One:

## Dimensions of the Orbital Debris Problem

This painting by Bill Hartman of the University of Arizona illustrates the major source of the orbital debris, explosions in space. Many accidental explosions of upper stages and spacecraft batteries, and some deliberate explosions, account for more than half of the almost 8000 objects that are cataloged. Through cooperative international efforts, most upper stage operations have been modified their to preclude explosions by venting all stored energy fuels and gasses.

# Chapter 1: The Current Environment

## Introduction

The meteoroid, or natural debris, environment has historically been a spacecraft design consideration. Meteoroids are part of the interplanetary environment and sweep through Earth orbital space at an average speed of 20 km / sec. Observational data indicate that, at any given instant in one time, a total of about 200 kg[46] of meteoroid mass is within 2000 km of the Earth's surface, the region containing the most-used orbits. Most of this mass is in meteoroids about 0.01 cm in diameter. This natural meteoroid flux varies in time as the Earth revolves about the Sun.

Man-made space debris (referred to as "orbital debris" throughout the rest of this document) differs from natural meteoroids because it remains in Earth orbit during its lifetime instead of passing through the space around the Earth. This study considers only the orbital debris environment and not reentering debris.

The estimated mass of man-made orbiting objects within 2000 km of the Earth's surface is about 2,000,000 kg.[45] These objects are in mostly high inclination orbits and pass one another at an average relative velocity of 10 km / sec (about 22,000 mph). Most of this mass is contained in about 3000 spent rocket stages, inactive satellites, and a comparatively few active satellites. A smaller amount of mass, about 40,000 kg, is in the remaining 4000 objects currently being tracked by space surveillance sensors.

Most of these smaller objects are the result of over 115 on-orbit fragmentations and 20 anomalous events in which objects separate from spacecraft but the parent body remains intact (see Appendix 1 for a detailed list).[24] Scientists recently conducted a detailed analysis of hypervelocity impact pits from orbital debris on returned surfaces of parts replaced on the Solar Max satellite, the Long Duration Exposure Facility (LDEF), Eureca (European Retrievable Carrier), Hubble Space Telescope and other surfaces exposed in space. Their investigations result in an estimate of 1000 kg for the total mass for orbital debris smaller than 1.0 cm and 300 kg for orbital debris smaller than 0.1 cm. The deduced distribution of mass and relative velocity is sufficient to cause the orbital debris environment to be more hazardous than the meteoroid environment to most spacecraft operating in Earth orbit below 2000 km. There is also clear evidence of unidentified sources of small debris in elliptical orbits.[58]

Information about the current debris environment is limited by the inability to track and catalog small objects. Although the mission of the Space Surveillance Network (SSN) is to track all man-made orbiting objects, technological and natural constraints serve to limit the effective tracking of objects smaller than 10 cm. Further, fiscal limitations limit the alternatives for modifying existing sensors or adding new systems.

This report is intended for internal agency and interagency planning purposes only. New programs or activities aimed at modifying existing systems or constructing new ones recommended in this report do not reflect Administration approval and must compete for funding in the budget process.

## I. Description of the Space Environment

### A. Background

Three types of orbital debris are of concern.

(1)Objects larger than 10 cm in diameter which are commonly referred to as large objects. These large objects are routinely detected, tracked, and cataloged.

(2)Objects between 1 and 10 cm in diameter which are commonly referred to as risk objects. Risk objects cannot be tracked and cataloged. Depending on their relative impact velocities, risk objects can cause catastrophic damage.

(3)Objects smaller than 1 cm in diameter are most commonly referred to as small debris or in some sizes microdebris.

The population of debris objects smaller than 10 cm is derived from statistical measurements made either in situ or from ground-based sensors.

The interaction among these three classes of objects combined with the long residual times in orbit of the larger fragments leads to further concern that there may be collisions producing additional fragments and causing the total debris population to grow.

The space around the Earth is generally divided into four orbital regimes:

(1) Low Earth Orbit (LEO) - defined by objects orbiting the Earth at less than 5500 km altitude; this equates to orbital periods of less than 225 minutes.
(2) Medium Earth Orbit (MEO) - defined by objects orbiting the Earth between LEO and GEO altitudes.
(3) Geosynchronous Earth Orbit (GEO) - defined by objects orbiting the Earth at an altitude of approximately 36,000 km; this equates to an orbital period of approximately 24 hours.
(4) Other - defined by highly eccentric and transfer orbits that transit between LEO and higher orbital altitudes.

Within these four regimes, orbits can be characterized as:

(1) Circular - the object remains at a near constant distance from the center of the Earth for its entire orbit. The object's velocity remains constant throughout each revolution of the Earth. Circular orbits are special cases of the more general elliptical orbits and only "approximate" true circles. Most large objects are in circular orbits.
(2) Elliptical - the object's distance from the center of the Earth varies as it follows the shape of an ellipse during each revolution. The closest point of approach to the Earth is called the object's perigee; the farthest point from the Earth is called the object's apogee. Objects achieve maximum velocity at perigee and achieve minimum velocity at apogee. Most fragmentation debris is in elliptical orbits, making it more difficult to acquire and track.

The greatest number of tracked objects are in LEO, the next greatest are in GEO, and the remaining objects are in MEO. Two navigation systems (the U.S. Global Positioning System (GPS) and Russian Global Navigation Satellite System (GLONASS) satellite constellations) are the first major users of MEO. There are a large number of upper stages used to deliver spacecraft to geosynchronous orbit and to the MEO orbits that are tracked in deeply elliptical orbits. The Russian Molniya spacecraft also use a deeply elliptical orbit.

The altitude distribution of objects tracked in orbit is illustrated in Figure 1. Equivalent objects referenced in the figure are defined as the average number of objects that can be observed in the altitude bin at any given instant in time. The limiting size is a function of the altitude of the orbit varying from 10 cm radar cross section in LEO to 1 m at geosynchronous altitudes. The peak population is near 1000 km orbital altitude where the population is about 100 objects in a 10 km altitude band. At 350 to 500 km orbital altitude where the International Space Station will operate, the population is about 10 objects in a 10 km altitude band. As noted in the figure, the distribution of objects by altitude is not uniform. There are peak usages in LEO for observation

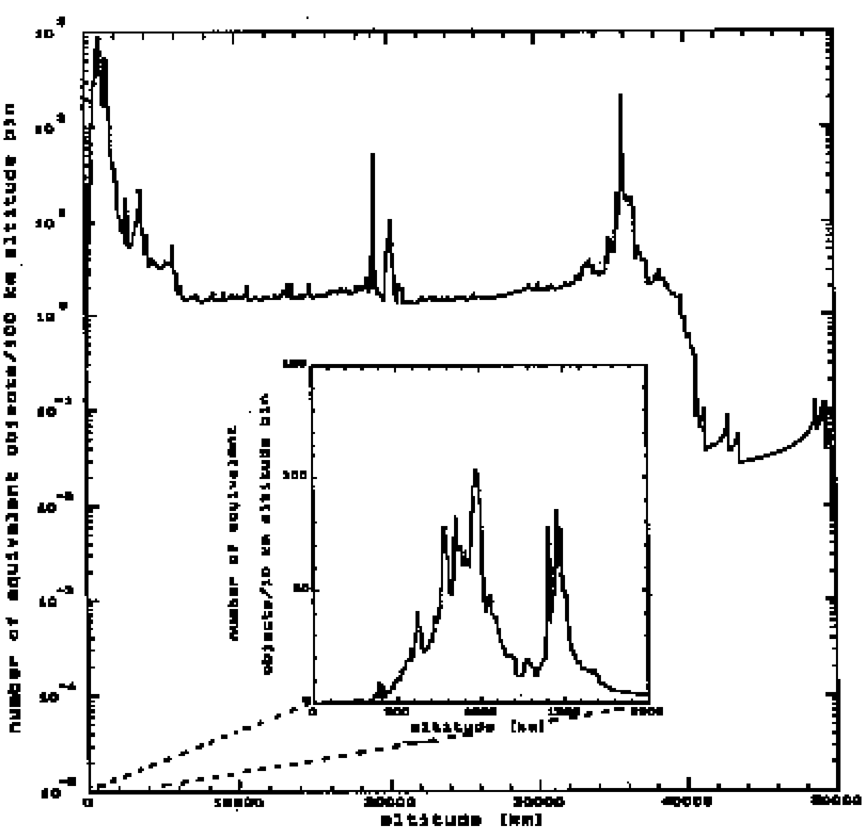


**Figure 1. Distribution of Satellites in Earth Orbit**

satellites, in MEO for navigation satellites, and in geosynchronous orbits for communications satellites.

Figure 2 shows a “snapshot” of the geographic distribution of tracked objects in GEO by their longitude. Most objects along the 0-degree latitude (equator) band are maintained in geostationary orbit. The other objects, rocket bodies and spacecraft no longer actively controlled, have a slightly inclined orbit which causes them to trace a figure-eight pattern on the ground about a point on the equator, traversing from the northern to the southern hemisphere and completing the pattern once every 24 hours.

### B. Debris Distribution

U.S. Space Command (USSPACECOM) presently maintains a catalog of more than 7000 objects in space. The great majority of these cataloged objects are low Earth orbiting objects and are approximately 10 cm apparent radar cross section or larger. Due to sensor characteristics, as the altitude increases so does the size of the smallest detectable objects. Radar cross section and physical size are the same value only for a sphere; since the shapes of the debris fragments are unknown, the most conservative assumption is that they approximate spheres. The breakdown of the cataloged objects, indicated by Table 1, reveals the relative distribution of the objects by altitude as of November 1, 1995.

**Table 1. Cataloged Objects by Altitude Ranges**

| Orbit Type | LEO | MEO | GEO | Other | Total |
|---|---|---|---|---|---|
| Cataloged Objects | 5747 | 134 | 601 | 1447 | 7929 |

There is a well-characterized cataloged population of more than 7000 objects that accounts for the largest fraction of the mass on orbit. There are sample measurements by radar and optical sensors and returned surfaces from space that indicate the number of cataloged objects are a small percentage of the total debris population larger than 1 mm. Table 2 shows the estimated debris population from both a numeric and mass-on-orbit perspective.

Small debris are the product of the breakup events noted above. Most of the fragments are too small to be routinely tracked by the SSN; their number must be estimated from other observations. Telescopic observations using the Ground Electro-Optical Deep Space System (GEODSS), Massachusetts Institute of Technology Lincoln Laboratory Experimental Test System (MIT/ LLETS), NASA Charged Coupled Device System

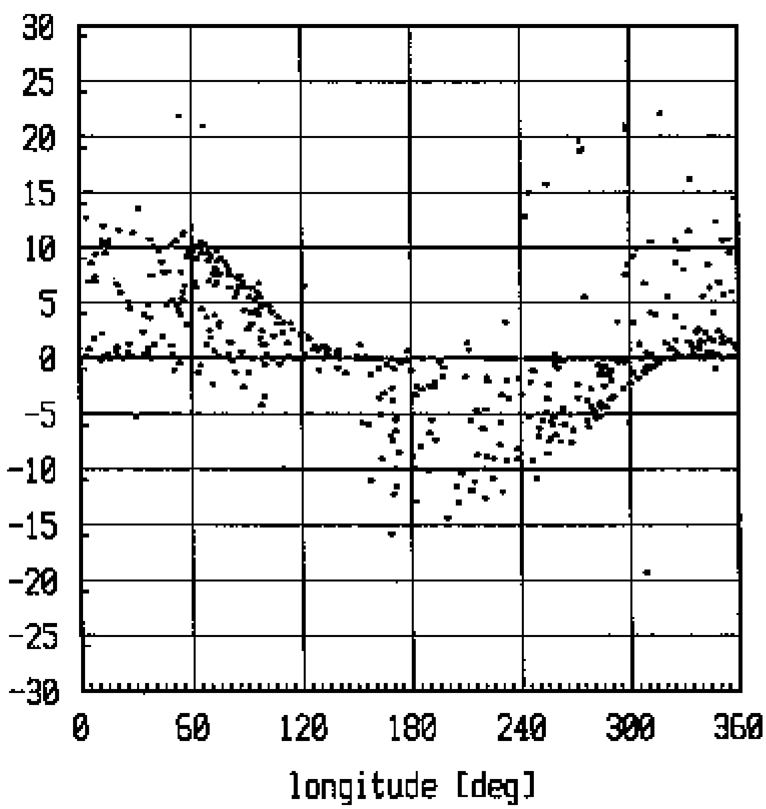


**Figure 2. Distribution of Objects In and Near Geosynchronous Earth Orbit**

(CCDS) and some European telescopes combined with the Haystack and Goldstone radars, and the examination of materials returned from space provide data samples which form the basis for statistical models of the debris environment. These environmental models contain submodules for simulating breakup events. These events include explosions or collisions at varying energy levels. Assumptions about the number and type of breakup events lead to modeled or predicted detection rates for special optical or radar sensors and impact rates for spacecraft surfaces exposed to the space debris environment. Figure 3 illustrates the particle distribution expected from each type of event. As expected, the few large fragments account for most of the mass while the many smaller fragments account for a large number of ejected debris particles.

**Table 2. Estimated Debris Population**

| Size | Number of Objects | % number | % Mass |
|---|---|---|---|
| >10 cm | 8,000 | 0.02% | 99.93% |
| 1-10 cm | 110,000* | 0.31% | 0.035%* |
| 0.1-1 cm | 35,000,000* | 99.67%* | 0.035%* |
| Total | 35,117,000* | 100.0%* | 2,000,000 kg# |

* statistically estimated values
\# calculated value from reported data

In addition to the 8000 cataloged objects, based on the statistical samples, it is estimated that there are several million objects between 0.1 and 1 cm and more than a hundred thousand between 1.0 cm and 10 cm.

### C. Orbital Lifetime

An orbiting object loses energy through friction with the upper reaches of the atmosphere and various other orbit perturbing forces. Over time, the object falls into progressively lower orbits and eventually falls to the Earth. As the object's potential energy (represented by its altitude) is converted to kinetic energy (energy due to its velocity), orbital velocity must increase as the altitude decreases. As an object's orbital trajectory draws closer to Earth, it speeds up and outpaces objects in higher orbits. In short, a satellite's orbital altitude decreases gradually while its orbital speed increases. Once an object enters the measurable atmosphere, atmospheric drag will slow it down rapidly and cause it to either burn up or deorbit and fall to Earth.

In LEO, unless reboosted, satellites in circular orbits at altitudes of 200 to 400 km reenter the atmosphere within a few months. At 400 to 900 km orbital altitudes, orbital lifetimes range from years to hundreds of years depending upon the mass and area of the satellite. Satellite Earth-orbit lifetimes are a function of atmospheric density and ballistic coefficients. The more mass per unit area of the object, the less the object will react to atmospheric drag. For example, a fragment with a large area and low mass (e.g., aluminum foil) will decay much faster (and hence a shorter orbital life) than a fragment with a small area and a high mass (e.g., a ball bearing). The combination of a variable atmosphere and unknown ballistic coefficients of space objects makes decay and reentry prediction difficult and inexact.

Orbital lifetimes for objects in elliptical orbits can vary significantly from lifetimes of objects in circular orbits. For elliptical orbits, the lower the perigee altitude, the greater the atmospheric drag effects. Therefore, considering a circular and an elliptical orbit with the same average altitude, an object in an elliptical orbit will have a higher apogee decay rate and a shorter on-orbit lifetime. If the elliptical orbit perigee height is equal to the circular orbit altitude, the circular orbit will decay faster because it is subject to the denser atmosphere during all of its orbital period.

The natural decay of earth-orbiting debris is also greatly affected by the 11-year solar cycle. The previous solar cycle peaked in 1981 and was above average in solar activity. The current solar cycle, peaked in 1991, and has also been associated with greater atmospheric drag and enhanced natural decay rates. High solar activity heats the Earth's upper atmosphere, which then expands and extends to higher altitudes. With this heating, the upper atmosphere density increases, causing satellites and debris to decay more rapidly. As a result, the debris population changes with solar activity depending on altitude and size. Above 600 km, the atmospheric density is already so low that the change in density does not noticeably affect the debris population, but below 600 km there are very noticeable changes. Over the course of the average 11-year solar sunspot cycle, the Earth's atmosphere is excited and rises significantly above its median altitude. However, this natural process of "cleansing" (during the entire solar cycle) is slow above 600 km and alone cannot offset the present rate of debris generation. Figure 4 illustrates the influence of the solar cycle on orbital lifetime of a typical spacecraft as a function of altitude.

In some high altitude orbits, there are significant effects due to the tidal influence of the Moon and the Sun. In some cases, these forces can

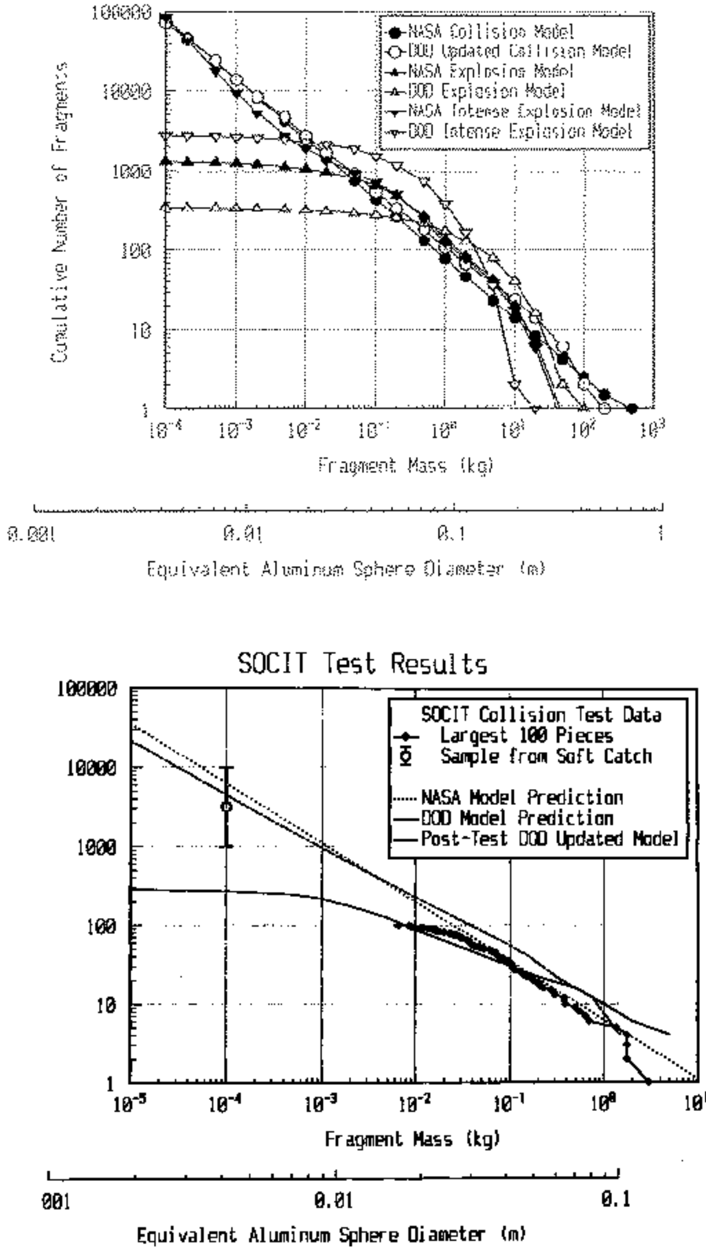


(a)

(b)

**Figure 3. Alternative Models of explosion and collision fragment distribution are illustrated in frame a, and the test and model distribution for hypervelocity collision are illustrated in frame b. The Satellite Orbital Debris Characterization Impact Test (SOCIT) was a series of laboratory tests impacting small spacecraft with a 150-g aluminum sphere at 6ms in a test chamber.**

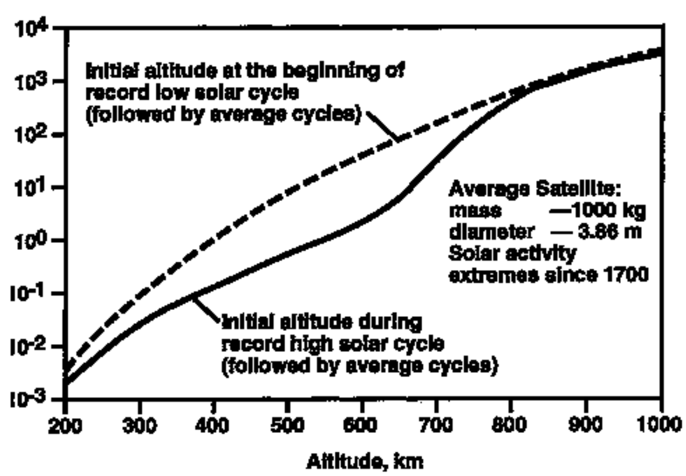


**Figure 4. Influence of Solar Cycle on Orbital Lifetime of a Spacecraft as a Function of Altitude**

be used to accelerate the decay of geosynchronous transfer orbit (GTO) debris. They also cause the north-south migration of objects in geosynchronous orbit that are not station-kept. In geosynchronous orbit and MEO, there are no significant natural cleansing forces.

Objects in geosynchronous orbit have orbital lifetimes in excess of a million years. Once released from station-keeping the solar and lunar forces cause the object to migrate through a region roughly 22,000 km north to south (from 15 degrees north to 15 degrees south) and 52 km above and below the geosynchronous arc. Terrestrial gravitational influences cause migration east and west around the Earth. The net effect of these motions is to create a torus around the Earth which contains 600 billion $km^3$ in which approximately 500 satellites are either actively station-kept or are derelicts drifting under the influence of the perturbing forces. The average distance between satellites is in excess of 60,000 km except for a few spacecraft that are kept at a particular longitude and actively controlled.

### D. Debris Effects

The effects of orbital debris impacts depend on velocity, angle of impact, and mass of the debris. Throughout this document, all orbital debris is assumed to be of the same material composition; thus, mass and particle diameter will be used interchangeably. For spacecraft design, it is useful to distinguish three debris size ranges:

(1) Sizes below 0.01 cm
(2) Sizes 0.01 cm to 1 cm
(3) Objects larger than 1 cm

For debris of sizes less than about 0.01 cm, surface pitting and erosion are the primary effects. Over a long period of time, the cumulative effect of individual particles colliding with a satellite might become significant since the number of particles in this size range is very large in LEO. Debris of sizes 0.01 cm to 1 cm produce significant impact damage which can be serious, depending upon system vulnerability and defensive design provisions. Objects larger than 1 cm can produce catastrophic damage.

For debris larger than about 0.1 cm, structural damage to the satellite becomes an important consideration. The kinetic energy in an aluminum sphere with a diameter of 1.3 mm at 10 km/second is the same as that in a 22 caliber long rifle bullet.

It is currently practical to shield against debris particles up to 1 cm in diameter, a mass of 1.46 grams or 0.05 ounces. For larger sizes of debris, current shielding concepts become impractical. Advanced shielding concepts may make shielding against particles up to 2 cm diameter reasonable, but it is possible that the only useful alternative strategy for large particles will be avoidance. While such a collision avoidance system is feasible, none is currently planned. For average size spacecraft, the number of particles larger than 10 cm is still small enough that a collision with them is unlikely. For very large spacecraft, collision probabilities are sufficiently high that an alternate means of protection may eventually be required.

Since debris damage is a function of relative velocity and the velocities at geosynchronous altitudes are relatively low, 1/10th those in LEO, the consequences are less dramatic, yet could still be significant. The danger of impact is also much lower due to the smaller number of objects and the larger region in which they orbit.

### E. Uncertainty in the Orbital Debris Environment

Figure 5 illustrates the data used to define the orbital debris environment. As noted in the figure, the only continuous source of data is the SSN observations. All other data sources, whether they are the special radar or optical observations or returned surfaces, are statistical sample measures. These techniques are the only means available to measure the smaller objects in orbit. The returned materials can be analyzed to determine the chemistry of the event and identify the proportion of man-made as opposed to natural meteoroids in the very small objects. The observations are then mathematically modeled to define the environment expected for future observations.

The illustration in Figure 6 represents the present state of understanding as measured or estimated from various data sources. It is intended to present a visual picture where the overlapping figures indicate areas where the various instruments can observe similar objects.

In this figure, the outer circle contains all natural and man-made debris of all sizes. The next circle inside is all man-made debris (down to .01 cm). Of all man-made debris, the cataloged objects are shown within the central circle around the typical 10 $m^2$ spacecraft and, as discussed previously, the LEO population consists primarily of objects larger than 10 cm observable by radars. This population has been maintained continuously for the last 30 years and is the best known portion of the population. There are other observations which have been conducted periodically to make measures below the threshold of routine maintenance.

Periodically since 1983, NASA has conducted a series of special observation campaigns using such optical systems as the ETS and GEODSS at Maui

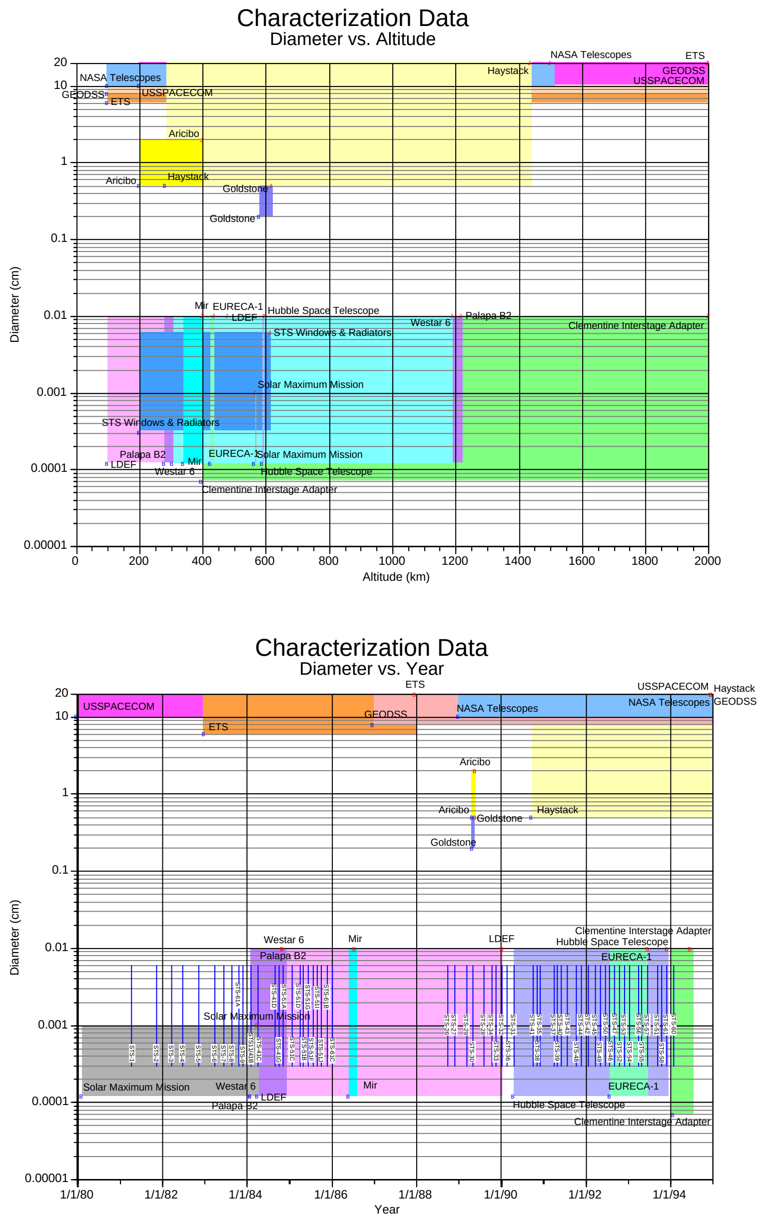


**Figure 5. Data Sources for the Definition of the Space Environment**

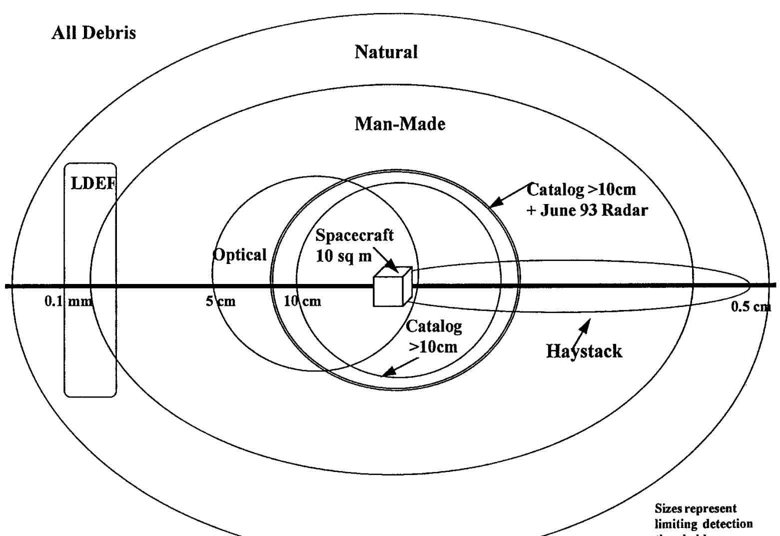


**Figure 6. The Relationship of Various Data Acquisition Sources to Each Other and the Natural and Man-Made Environment**

and Diego Garcia; a portable CCD telescope at Black Birch, New Zealand, and Rattlesnake Mountain, Washington; and such radars as Goldstone and Arecibo. These observations indicated that there were orbiting objects that were more readily observed optically than by radar.

During June 1993, a special debris search campaign was conducted by the Air Force Space Command (AFSPC) to test the ability of the network to detect smaller objects with the current sensors, making concurrent radar and optical measurements. Roughly 1000 additional tracks were observed by increasing the sensitivity of the network. This led to the identification of approximately 100 new objects. This is represented in Figure 6 by the double circle outside the catalog circle.

To detect still smaller objects, observations have been made with more sensitive instruments which of necessity have smaller fields of view. The optical systems have fields of view ranging from 1 to 6 degrees while the most sensitive radars have fields of view of a few hundredths of a degree.

The optical systems used by the Department of Defense (DOD) are capable of seeing about 80% of the cataloged objects. During the June 1993 campaign, the percentage of newly detected objects revealed that 40% of these unknown new objects in LEO were not in the catalog. Further analysis showed that only 10 to 15% of the unknowns were seen by both radar and optical devices. Therefore, the optical circle in Figure 6, which overlaps 80% of the catalog population, is 40% larger and overlaps 10 to 15% of the double circle. Some objects have poor radar reflectivity but good optical reflectivity or the converse because of the materials properties and the shape of the object.

The Haystack radar observations provide another significant source of data. The Haystack radar, while it can certainly see most cataloged objects, has concentrated on seeing small debris, the majority of which is uncataloged. Because of the extreme sensitivity of the Haystack radar, it can also see some natural meteoroid debris passing close to the Earth. The elliptical shape of the Haystack figure indicates that it is sampling a small portion of the total population. The Goldstone radar is also used to make measurements of the small debris population.

In addition to all these ground-based remote measurements, objects returned from space have allowed us to sample impacts from very small debris (0.1 cm and smaller) and obtain a sample measurement of the ratio of man-made to natural debris in very low Earth orbit. The shape of the LDEF region in Figure 6 is symbolic of the distribution of the measured impact craters on exposed surfaces, none of which were observable from the ground but represented both man-made and natural impact events.

## II. Sources of Orbital Debris

### A. General

The U.S. and Russia have contributed in roughly equal proportions to the orbital debris environment. Figure 7 shows a steady growth in

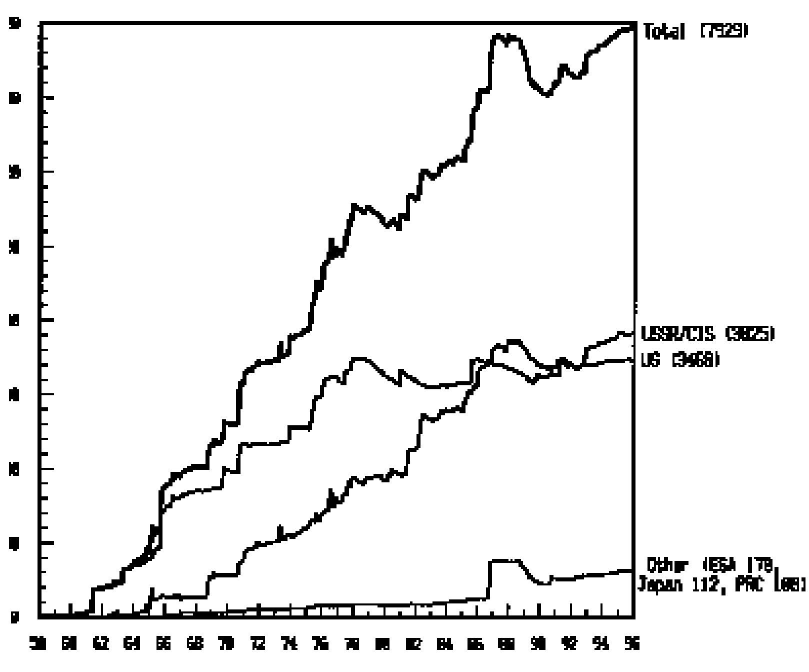


**Figure 7. The Number of Catalogued Satellites in Orbit by Nation of Origin**

the cataloged satellite population over the past 30 years. Only during the periods 1978 through 1981 and 1989 through 1992 did the catalog growth rate decline. This decline in the growth rate resulted from an expansion of the upper atmosphere caused by a strong solar maximum. The atmospheric expansion significantly accelerated the decay of satellites and debris in orbits below about 600 km.

Satellite fragmentations (see para. II.B.) are the primary source contributing to the increase in the number of cataloged Russian objects which started in 1993. Similarly, the single breakup of a French Ariane rocket body in 1986 is the source of the increase in the number of "Other" cataloged objects shown in Figure 7.

Operational spacecraft represent only 5% of the cataloged objects in Earth orbit. The remainder constitute varying types of orbital debris in four general categories:

(1) Operational Debris
(2) Fragmentation Debris
(3) Deterioration Debris
(4) Solid Rocket Motor Ejecta

## B. Operational Debris

Operational debris is composed of inactive payloads and objects released during satellite delivery or satellite operations, including lens caps, separation and packing devices, spin-up mechanisms, empty propellant tanks, spent and intact rocket bodies, payload shrouds, and a few objects thrown away or dropped during manned activities. This class of debris is diminishing as designs are adopted which no longer release such objects. Of the cataloged objects in Earth orbit, 95% can be considered orbital debris as opposed to operational spacecraft.

Table 3 presents the altitude distribution of the sources of tracked objects discussed above. As shown by the table, the majority of tracked objects are in LEO. This is an indication both of the capabilities of the tracking sensors and the level of space activity in LEO.

**Table 3. Cataloged Objects by Altitude Regime**

| | SPACECRAFT | ROCKET BODIES | DEBRIS FRAGMENTS | TOTAL |
|---|---|---|---|---|
| LEO | 1292 | 712 | 3743 | 5747 |
| MEO | 107 | 24 | 3 | 134 |
| GEO | 465 | 133 | 3 | 601 |
| Transfer | 75 | 276 | 147 | 498 |
| Other | 359 | 361 | 229 | 949 |
| TOTAL | 2298 | 1506 | 4125 | 7929 |

## C. Fragmentation Debris

Of particular concern is the sustained rate of fragmentation events despite the active efforts of spacefaring nations to reduce the probability of such events by making all their systems passive at

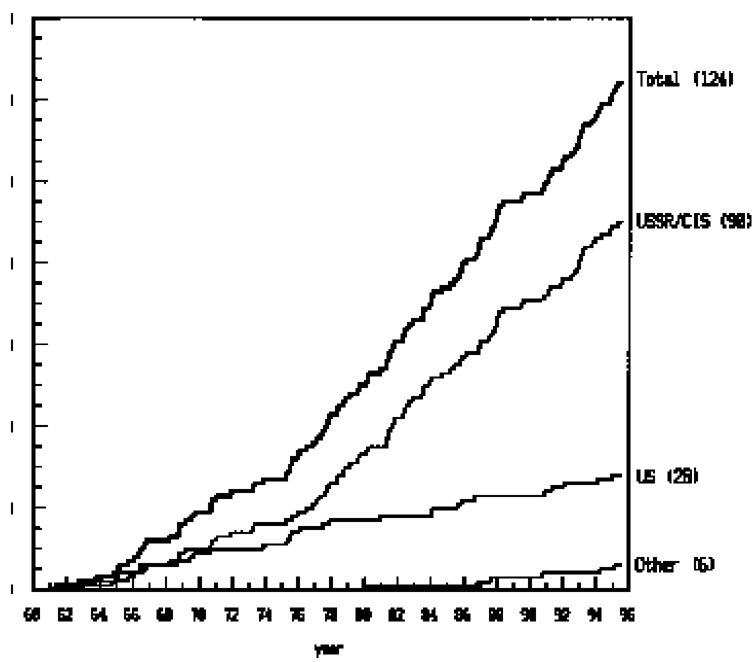


**Figure 8. History of Fragmentation Events**

mission end by expelling residual propellants and other forms of stored energy. Figure 8 indicates the cumulative number of breakup events by year (see Appendix 1).

In the past 4 years, there have been 19 breakup events. Three of these involved spacecraft and the other 16 were rocket bodies, many being the booster units of the Russian Proton D-1 stage. Figure 9 illustrates the number of fragmentations by year since 1961. Despite the introduction of procedures to eliminate stored energy, there has not yet been a change in the rate of breakups.

Since the first detected fragmentation of the Omicron rocket body in June of 1961, 124 fragmentation events have been documented. These fragmentation events serve as the dominant mechanism in the creation of larger sizes of debris. Generally, fragmentations may result from either explosions or collisions. There are several explosive mechanisms including: (1) the catastrophic failure of internal components such as batteries, (2) propellant-related explosions (high energy explosions), (3) failure of pressurized tanks (low energy explosions), and (4) intentional destruction. Fragmentation may also be caused by collisions with other orbital objects, although no such events have been confirmed. Each type of event produces a characteristic size and velocity distribution of the resulting debris cloud. For example, low energy explosions typically produce fewer small objects than high energy explosions. In LEO, a hypervelocity collision would typically produce many more small objects than a high energy explosion since the impact and resultant shock wave melts and vaporizes satellite materials. A prominent example of high energy explosions is the Delta rocket body breakups in LEO. As a class, debris from these breakups dominate the catalog.

Figure 10 shows a Gabbard diagram of a recent Delta rocket body breakup. Gabbard diagrams are used to identify and analyze breakup events. In the diagram, the apogee and perigee of each object are shown by a pair of points. Fragments that receive a posigrade impulse are distributed along the right side of the diagram and retain their original perigee altitude. Conversely, pieces receiving retrograde impulses are distributed to the left and retain their original apogee altitudes. The original rocket body

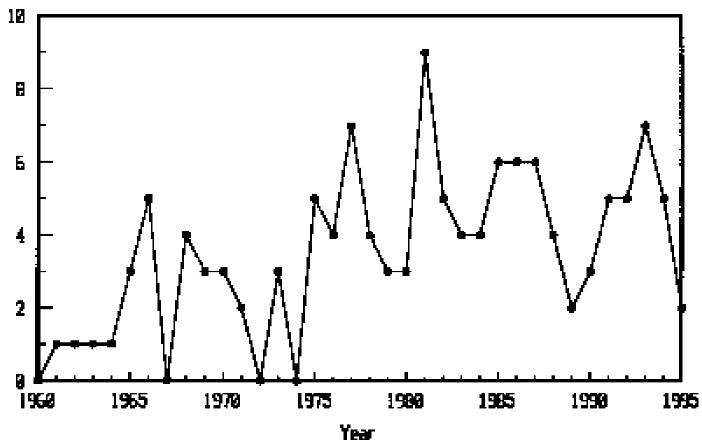


**Figure 9. Number of Breakup Events by Year of Occurrence**

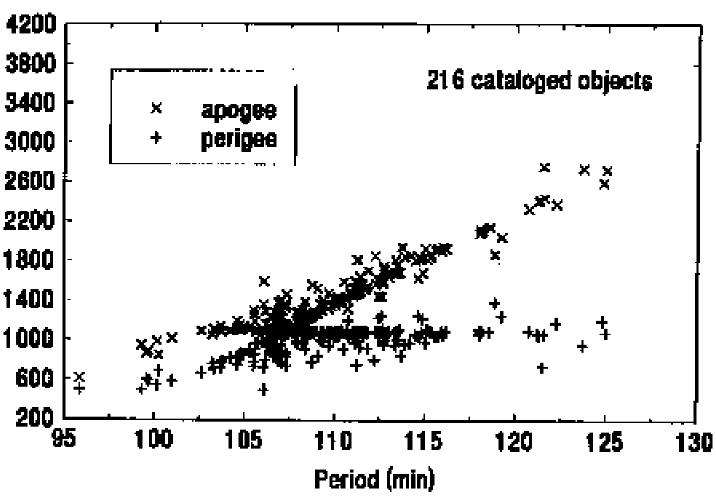


**Figure 10. Gabbard Diagram of the Breakup of Nimbus 6 Delta Second Stage**

was located at the center of the cross. This cross is characteristic of breakups from near circular orbits. The collapse of the left arm of the Gabbard is indicative of the cleansing effect of atmospheric drag on the objects with lower perigees. Moreover, the diagram illustrates that breakup events distribute debris over a wide range of altitudes.

Two fragmentation events appear to have taken place in GEO. Also, nonoperational satellites in GEO are frequently not tracked for long periods of time during which unobserved fragmentations could occur. In the absence of data to the contrary, it is believed that there is not a significant number of objects in GEO to create a problem at this time.

The causes of many fragmentations (22%) remain unknown, in part, due to the limited data available for analysis. Table 4 lists the causes of fragmentations as currently known.

**Table 4. Causes of Satellite Fragmentations**

| Cause | % of Events | % Fragments Still in Orbit |
|---|---|---|
| Unknown | 22 | 43 |
| Propulsion Related | 36 | 42 |
| Deliberate | 38 | 13 |
| Systems Related * | 4 | 2 |

* Electrical, command and control systems

### D. Deterioration Debris

Very small debris particles are created by the gradual disintegration of spacecraft surfaces as a result of exposure to the space environment. This deterioration includes paint flaking and plastic and metal erosion. It has been hypothesized that paint flaking is caused by the erosion of organic binders in the paint due to exposure to atomic oxygen. The dramatic consequences of even small paint flakes can be seen in the widely reported impacts on the Space Shuttle window.[54]

Deterioration debris is not limited exclusively to the smaller objects. Several orbital objects have been observed to periodically shed materials over long periods of time. Much of this material may be deteriorating thermal blankets and insulation. Examples include debris from the U.S. Snapshot payload / rocket body complex, Ariane upper stages, and Russian Proton upper stages in GTO.

### E. Solid Rocket Motor Ejecta

Solid rocket motors (SRMs) typically are used to transfer objects from LEO to GEO, and they eject thousands of kilograms of aluminum oxide dust into the orbital environment. This ejected dust is very small, with characteristic sizes believed to be less than 0.01 cm. Nonetheless, long-term exposure of payloads to such particles is likely to cause erosion of exterior surfaces, chemical contamination, and may degrade operations of vulnerable components such as optical windows and solar panels. Recent chemical analysis of impacts on LDEF indicates that a significant fraction of the impact craters contain traces of aluminum. In some cases, larger chunks of unburned SRM propellant or slag may be released (ignited propellant will not burn completely outside the pressurized confines of the rocket body). Some of these chunks may be released long after the completion of the burn.

Since SRM particles are ejected in the rocket plume, most have very large retrograde velocities (~3 km / s). This fact, combined with the low mass of the dust and low altitude parking orbits used in current mission profiles, will cause the particles to decay very rapidly, probably within a few perigee passages. Those that do not quickly reenter are dispersed by solar radiation pressure. Thus, the operational threat of SRM dust is probably limited to brief periods of time related to specific mission events. Even the majority of the ejecta from the GPS SRM semi-synchronous insertion burns has a perigee height at or below the Earth’s surface.


The Haystack radar located near Boston, Massachusetts, has been used to monitor the orbital debris population for the past four years. It is operated in an unconventional mode: the antenna is fixed, and debris objects that fly through the radar beam are detected. This radar is one of the most powerful in the world, and is capable of detecting 1-cm objects orbiting at 1000-km altitude. Measurements with this radar have provided the best and most complete picture available of the small debris population.